Fluid Dynamics and Mass Transfer in the Total Capacity Range of Packed Columns up to the Flood Point

R. Billet and M. Schultes*

Up to now, the only equations that were known for calculating mass transfer during two-phase countercurrent flow in packed columns were those that apply to the range extending up to the loading point. The gas and liquid streams flow separately through the column below but not above this point. Above it, the shear stress in the gas stream supports an increasing quantity of liquid in the column, with the result that the liquid holdup greatly increases. Finally, at the flood point, the liquid accumulates to such an extent that column instability occurs. Mass transfer in this upper loading range can be described if these fluid dynamic relationships are taken into consideration. The algorithm that is presented here for its prediction is based on theoretical and experimental studies.

1 Fluid Dynamics

A model that describes the fluid dynamic relationships in packed columns with countercurrent flow of the gas and liquid phases was developed in a previous work by Billet [1–3]. It allows the flow conditions to be described up to the flood point. The assumption made was that the void fraction in a bed of packing could be represented by a multiplicity of vertical channels through which the liquid flows downwards in the form of a film countercurrent to the ascending gas stream. This model also permits mass transfer in the loading range up to the flood point to be determined.

If a gas flows countercurrent to a liquid film and the inertia forces are neglected, the shear and gravity forces at the surface of the film $s = s_0$, as defined by Eq. (1), are in equilibrium with the shear forces τ in the gas stream in accordance with Eq. (2)[1],

$$\frac{\mathrm{d}\left(\eta_\mathrm{L}\dfrac{\mathrm{d}\bar{u}_{\mathrm{L},s}}{\mathrm{d}s}\right)}{\mathrm{d}s} = -\varrho_\mathrm{L}\cdot g \tag{1}$$

$$\tau = -\psi_\mathrm{L}\frac{\varrho_\mathrm{V}\bar{u}_\mathrm{V}^2}{2} \tag{2}$$

where $\bar{u}_{\mathrm{L},s}$ is the local liquid velocity in the film, η_L is the dynamic viscosity of the liquid, ϱ_L is the density of the liquid, g is the acceleration due to gravity, $\bar{u}_\mathrm{V}$ is the average effective gas velocity, ϱ_V is the gas density, and ψ_L is the resistance factor for two-phase flow.

It follows from this that the local velocity $\bar{u}_{\mathrm{L},s}$ is given by

$$\bar{u}_{\mathrm{L},s} = \left(\frac{\varrho_\mathrm{L}}{\eta_\mathrm{L}}g s_0 - \psi_\mathrm{L}\frac{1}{\eta_\mathrm{L}}\frac{\bar{u}_\mathrm{V}^2}{2}\varrho_\mathrm{V} - \frac{1}{2}\frac{\varrho_\mathrm{L}}{\eta_\mathrm{L}}g s\right)s \tag{3}$$

and the average effective liquid velocity in the film $\bar{u}_\mathrm{L}$, by

$$\bar{u}_\mathrm{L} = \frac{1}{s_0}\int_{s=0}^{s=s_0}\bar{u}_{\mathrm{L},s}\,\mathrm{d}s = s_0\frac{1}{\eta_\mathrm{L}}\left(\frac{1}{3}\varrho_\mathrm{L}g s_0 - \frac{1}{4}\psi_\mathrm{L}\bar{u}_\mathrm{V}^2\varrho_\mathrm{V}\right) \tag{4}$$

The loading point in two-phase countercurrent flow is reached whenever the gas velocity is just so high that $\bar{u}_{\mathrm{L},s}$ becomes zero at the surface of the film $s = s_0$. In view of this fact, Eq. (5) can be derived from the void fraction ε, the specific surface a of the bed of packing, and the liquid holdup $h_\mathrm{L} = s_0 a$ corresponding to the gas velocity at the loading point $u_{\mathrm{V,S}}$. The term ψ_S for the resistance factor in Eq. (5) is described by Eq. (6); and that for the liquid holdup $h_{\mathrm{L,S}}$ by Eq. (7). In the derivation of Eq. (5), the terms $u_\mathrm{V} = \bar{u}_\mathrm{V}(\varepsilon - h_\mathrm{L})$ and $u_\mathrm{L} = \bar{u}_\mathrm{L}h_\mathrm{L}$ were introduced to allow for the fundamental relationship between the superficial gas and liquid velocities u_V and u_L and the figures obtained for the average effective gas and liquid velocities $\bar{u}_\mathrm{V}$ and $\bar{u}_\mathrm{L}$ from Eqs (3) and (4) [2–5].

$$u_{\mathrm{V,S}} = \sqrt{\frac{g}{\psi_\mathrm{S}}(\varepsilon - h_{\mathrm{L,S}})}\sqrt{\frac{h_{\mathrm{L,S}}}{a}}\sqrt{\frac{\varrho_\mathrm{L}}{\varrho_\mathrm{V}}} \tag{5}$$

$$\frac{1}{\psi_\mathrm{S}} = C_\mathrm{S}^2\left(\frac{L}{V}\sqrt{\frac{\varrho_\mathrm{V}}{\varrho_\mathrm{L}}}\left(\frac{\eta_\mathrm{L}}{\eta_\mathrm{V}}\right)^{0.4}\right)^{2n_\mathrm{S}} \tag{6}$$

$$h_{\mathrm{L,S}} = \left(12\frac{1}{g}\frac{\eta_\mathrm{L}}{\varrho_\mathrm{L}}u_{\mathrm{L,S}}a^2\right)^{1/3} \tag{7}$$

The constant for the specific packing C_S and the exponent n_S in Eq. (6) depend on the mass flow rate L/V and density

* Prof. Dr.-Ing. R. Billet and Dr.-Ing. M. Schultes, Ruhr University Bochum, Universitätsstraße 150, D-4630 Bochum.

1) List of symbols at the end of the paper.

0930-7516/95/0612-0371 $5.00+.25/0

ϱ_V/ϱ_L ratios, in accordance with Eqs (8) and (9); and numerical values of C_S for the packings investigated are listed in Table 1 [4, 5].

If $\frac{L}{V}\sqrt{\frac{\varrho_V}{\varrho_L}} \leq 0.4$: $n_s = -0.326$; C_S from Table 1 (8)

If $\frac{L}{V}\sqrt{\frac{\varrho_V}{\varrho_L}} > 0.4$:

$$n_s = -0.723 \; ; \quad C_S = 0.695\, C_{S,\text{Tab. 1}} \left(\frac{\eta_L}{\eta_V}\right)^{0.1588} \tag{9}$$

Table 1a. Characteristic data and constants for dumped packings.

Dumped packings		Size [mm]	N [1/m³]	a [m²/m³]	ε [m³/m³]	C_S	C_{Fl}	C_L	C_V
Pall ring	Metal	50	6242	112.6	0.951	2.725	1.580	1.192	0.410
		35	19517	139.4	0.965	2.629	1.679	1.012	0.341
		25	53900	223.5	0.954	2.627	2.083	1.440	0.336
	Plastic	50	6765	111.1	0.919	2.816	1.757	1.239	0.368
		35	17000	151.1	0.906	2.654	1.742	0.856	0.380
		25	52300	225.0	0.887	2.696	2.064	0.905	0.446
	Ceramic	50	6215	116.5	0.783	2.846	1.913	1.227	0.415
Ralu flow	Plastic	No. 2	4750	100	0.95	3.412	2.174	1.270	0.330
Ralu ring	Plastic	50	5770	95.2	0.938	2.843	1.812	1.520	0.303
		50 hydr.	5720	95.2	0.939	2.843	1.812	1.481	0.343
NOR PAC ring	Plastic	50	7330	86.8	0.947	2.959	1.786	1.080	0.322
		35	17450	141.8	0.944	3.179	2.242	0.756	0.425
		25[6]	50000	202.0	0.953	3.277	2.472	0.883	0.366
		25[10]	48920	197.9	0.920	2.865	2.083	0.976	0.410
Hiflow ring	Metal	50	5000	92.3	0.977	2.702	1.626	1.168	0.408
		25	40790	202.9	0.962	2.918	2.177	1.641	0.402
	Plastic	50	6815	117.1	0.925	2.894	1.871	1.478	0.345
		50 hydr.	6890	118.4	0.925	2.894	1.871	1.553	0.369
		50 S	6050	82.0	0.942	2.866	1.702	1.219	0.342
		25	46100	194.5	0.918	2.841	1.989	1.577	0.390
	Ceramic	50	5120	89.7	0.809	2.819	1.694	1.377	0.379
		38	13241	111.8	0.788	2.840	1.930	1.659	0.464
		20	121314	286.2	0.758	2.875	2.410	1.744	0.465
Glitsch ring	Metal	30 PMK	29200	180.5	0.975	2.694	1.900	1.920	0.450
		30 P	31100	164.0	0.959	2.564	1.760	1.577	0.398
Glitsch CMR ring	Metal	1.5″	60744	174.9	0.974	2.697	1.841		
		1.5″ T	63547	188.0	0.972	2.790	1.870		
		1.0″	158467	232.5	0.971	2.703	1.996		
		0.5″	560811	356.0	0.952	2.644	2.178	2.038	0.495
TOP-Pak ring	Alu	50	6871	105.5	0.956	2.528	1.579	1.326	0.389
Raschig ring	Ceramic	50	5990	95.0	0.830	2.482	1.574	1.416	0.210
		25	47700	190.0	0.680	2.454	1.899	1.361	0.412
VSP ring	Metal	50	7841	104.6	0.980	2.806	1.689	1.222	0.420
		25	33434	199.6	0.975	2.755	1.970	1.376	0.405
Envi Pac ring	Plastic	80	2000	60.0	0.955	2.846	1.522	1.603	0.257
		60	6800	98.4	0.961	2.987	1.864	1.522	0.296
		32	53000	138.9	0.936	2.944	2.012	1.517	0.459
Bialecki ring	Metal	50	6278	121.0	0.966	2.916	1.896	1.721	0.302
		35	18200	155.0	0.967	2.753	1.885	1.412	0.390
		25	48533	210.0	0.956	2.521	1.856	1.461	0.331
Tellerette	Plastic	25	37037	190.0	0.930	2.913	2.132	0.899	
Hackette	Plastic	45	12000	139.5	0.928	2.832	1.966		
Raflux ring	Plastic	15	193522	307.9	0.894	2.825	2.400	1.913	0.370
Berl saddle	Ceramic	25	80080	260.0	0.680			1.246	0.387
		13	691505	545.0	0.650			1.364	0.232
DIN-PAK	Plastic	70	9763	110.7	0.938	2.970	1.912	1.527	0.326
		47	28168	131.2	0.923	2.929	1.991	1.690	0.354

Table 1b. Characteristic data and constants for regular packings.

Regular packings		Size [mm]	N [1/m³]	a [m²/m³]	ε [m³/m³]	C_S	C_{Fl}	C_L	C_V
Pall ring	Ceramic	50	7502	155.2	0.754	3.793	3.024	1.278	0.333
Bialecki ring	Metal	35	20736	176.6	0.945			1.405	0.377
Ralu pack	Metal	YC-250		250.0	0.945	3.178	2.558	1.334	0.385
Mellapak	Metal	250 Y		250.0	0.970	3.157	2.464		
Gempak	Metal	A2T-304		202.0	0.977	2.986	2.099		
Impulse packing	Metal	250		250.0	0.975	2.610	1.996	0.983	0.270
	Ceramic	100		91.4	0.838	2.664	1.655	1.317	0.327
Montz packing	Metal	B1-200		200.0	0.979	3.116	2.339	0.971	0.390
		B1-300		300.0	0.930	3.098	2.464	1.165	0.422
	Plastic	C1-200		200.0	0.954			1.006	0.412
		C2-200		200.0	0.900	2.653	1.973	0.739	
Euroform	Plastic	PN-110		110.0	0.936	3.075	1.975	0.973	0.167

Above the loading point, the shear stress in the countercurrent gas stream arrests the downward flow of the liquid film, with the result that the liquid holdup rapidly increases, as is illustrated in Fig. 1, which was compiled from experimental results. It can be seen from this diagram that the curves drawn through the plotted points become vertical at the flood point, and the condition $du_V/dh_L = 0$ can thus be formulated. Another boundary condition at the flood point, i.e. $du_L/dh_L = 0$, can be deduced from Fig. 2, which shows the results of studies on the change in liquid holdup with increase in the liquid load. These conditions allow Eqs (10) and (11) to be derived for the gas and liquid velocities at the flood point $u_{V,Fl}$ and $u_{L,Fl}$; and Eq. (12) for the liquid holdup $h_{L,Fl}$ if the L/V ratio is constant [3–5].

$$u_{V,Fl} = \sqrt{2}\sqrt{\frac{9}{\psi_{Fl}}\frac{(\varepsilon - h_{L,Fl})^{3/2}}{\varepsilon^{1/2}}}\sqrt{\frac{h_{L,Fl}}{a}}\sqrt{\frac{\varrho_L}{\varrho_V}} \tag{10}$$

$$u_{L,Fl} = \frac{9}{3}\frac{1}{a^2}\frac{\varrho_L}{\eta_L}h_{L,Fl}^3\left(1 - \frac{3}{2}\frac{\varepsilon - h_{L,Fl}}{\varepsilon}\right) \tag{11}$$

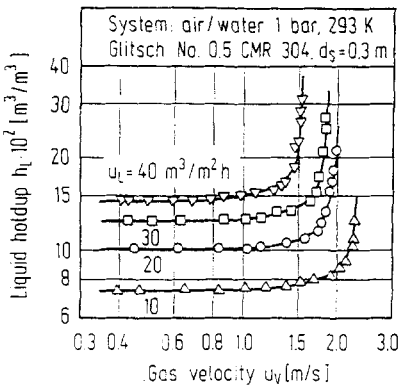

Fig. 1. Liquid holdup as a function of specific gas velocity for various liquid loads.

$$h_{L,Fl}^3(3h_{L,Fl} - \varepsilon) = \frac{6}{9}a^2\varepsilon\frac{\eta_L}{\varrho_L}\frac{L}{V}\frac{\varrho_V}{\varrho_L}u_{V,Fl} \tag{12}$$

The resistance factor at the flood point ψ_{FL} can be described by Eqs (13)–(15) in analogy to the loading point, although the effect of the viscosity ratio η_L/η_V is less. Once again, the constant C_{Fl} for the specific packing can be obtained from Table 1 [4, 5].

$$\frac{1}{\psi_{Fl}} = C_{Fl}^2\left(\frac{L}{V}\sqrt{\frac{\varrho_V}{\varrho_L}}\left(\frac{\eta_L}{\eta_V}\right)^{0.2}\right)^{2n_{Fl}} \tag{13}$$

$$\text{If } \frac{L}{V}\sqrt{\frac{\varrho_V}{\varrho_L}} \leq 0.4\text{: } n_{Fl} = -0.194\ ;\quad C_{Fl} \text{ from Table 1} \tag{14}$$

$$\text{If } \frac{L}{V}\sqrt{\frac{\varrho_V}{\varrho_L}} > 0.4\text{:}$$

$$n_{Fl} = -0.708\ ;\quad C_{Fl} = 0.6244\,C_{Fl,\text{Tab. 1}}\left(\frac{\eta_L}{\eta_V}\right)^{0.1028} \tag{15}$$

The liquid holdup at the flood point $h_{L,Fl}$ must be determined by iteration from Eq. (12) for the mass flow ratio L/V that relates to the problem in question. In this case, the only values of physical significance are those in the $\varepsilon/3 \leq h_{L,Fl} \leq \varepsilon$ range. The example given in Fig. 3 for the calculation of liquid holdup by means of Eq. (12) applies to a 25-mm plastic Pall ring and an air/water system. It can be seen that $h_{L,Fl}$ is only slightly greater than $\varepsilon/3$ over a wide range and does not increase significantly until the liquid load exceeds 200 m³/m² h.

2 Mass Transfer

The authors' comprehensive studies on mass transfer in packed columns have revealed that the volumetric mass transfer coefficients on the gas and liquid sides $\beta_L a_{Ph}$ and

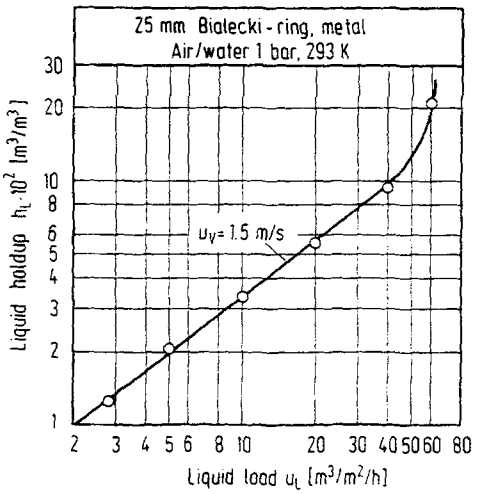

Fig. 2. Liquid holdup as a function of liquid load for constant gas velocity.

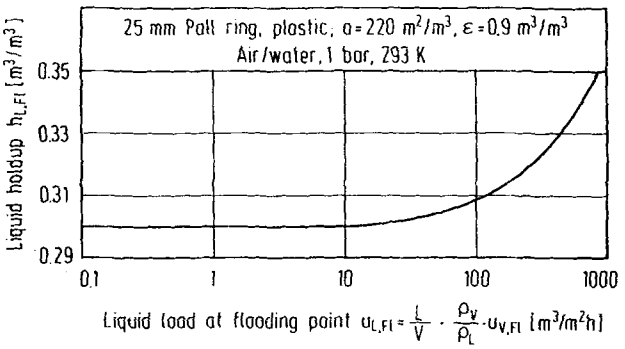

Fig. 3. Dependence of the liquid holdup as a function of liquid load for a 25 mm-plastic Pall ring.

$\beta_V a_{Ph}$ can best be described by Eqs (16) and (17) up to the loading point. The liquid holdup h_L, as described by Eq. (18), is included in the equations, because it is not a function of the gas velocity up to the loading point, i.e. $h_L = h_{L,S}$, as described by Eq. (7) [2, 6, 9, 10, 11],

$$\beta_L a_{Ph} = C_L \, 12^{1/6} \left(\frac{u_L}{h_L}\right)^{1/2} \left(\frac{D_L}{d_h}\right)^{1/2} a \left(\frac{a_{Ph}}{a}\right) \tag{16}$$

$$\beta_V a_{Ph} = C_V \frac{1}{(\varepsilon - h_L)^{1/2}} \frac{a^{3/2}}{d_h^{1/2}} D_V \left(\frac{u_V}{a \nu_V}\right)^{3/4} \left(\frac{\nu_V}{D_V}\right)^{1/3} \left(\frac{a_{Ph}}{a}\right) \tag{17}$$

$$h_L = \left(12 \frac{1}{g} \frac{\eta_L}{\varrho_L} u_L a^2\right)^{1/3} \quad \text{if} \quad u_V \leq u_{V,S} \tag{18}$$

where C_L and C_V are constants for specific packings, values of which are listed in Table 1, d_h is the hydraulic diameter, as defined by Eq. (19), D_L and D_V are the diffusion coefficients for the components transferred in the liquid and the gas, ν_L and ν_G are the kinematic viscosities of the liquid and the gas, and a_{Ph}/a is the effective area, as described by Eq. (20), of the phase boundary available for mass transfer expressed in terms of the area of the unwetted packing [6, 9, 10].

$$d_h = 4 \frac{\varepsilon}{a} \tag{19}$$

$$\frac{a_{Ph}}{a} = 1.5 \, (a \, d_h)^{-0.5} \left(\frac{u_L \, d_h}{\nu_L}\right)^{-0.2} \times \left(\frac{u_L^2 \, \varrho_L \, d_h}{\sigma_L}\right)^{0.75} \left(\frac{u_L^2}{g \, d_h}\right)^{-0.45} =$$

$$= 1.5 \, (a \, d_h)^{-0.5} \, Re_L^{-0.2} \, We_L^{0.75} \, Fr_L^{-0.45} \tag{20}$$

The height of a column is the product of the height of an overall transfer unit HTU_{OV} and the number of overall transfer units NTU_{OV} on the gas side (Eq. (21)). The NTU_{OV} can be calculated from the equilibrium curve, the operating characteristics, and the column inlet and outlet concentrations; and the HTU_{OV}, from the height of transfer units on the gas and liquid sides HTU_V and HTU_L and the stripping factor λ (Eq. (22)). The latter is the ratio of the slope of the equilibrium curve m_{yx} to the molar liquid/gas flow ratio $\dot{L}/\dot{V}$.

$$H = HTU_{OV} \, NTU_{OV} \tag{21}$$

$$HTU_{OV} = HTU_V + \lambda \, HTU_L = \frac{u_V}{\beta_V a_{Ph}} + \left(\frac{m_{yx}}{\dot{L}/\dot{V}}\right) \frac{u_L}{\beta_L a_{Ph}} \tag{22}$$

Eqs (16) and (17) for $\beta_L a_{Ph}$ and $\beta_V a_{Ph}$ were derived from physical considerations, and their validity has been confirmed in absorption, desorption, and rectification studies. Eq. (20) is valid for systems in which the surface tension σ_L remains approximately constant during mass transfer or for systems in which the surface tension of the liquid film increases along the length traversed in the column. If, however, the surface tension of the film decreases along the downward path in the column, vortices will occur at the phase interface and thus reduce the area of the phase boundary. This case is referred to as a negative system. Mass transfer experiments in rectification have demonstrated that allowance can be made for the resulting additional effect on the area of the phase boundary by means of the Marangoni number, as indicated by Eqs (23) – (25). A relationship for the area of the phase boundary is thus obtained (Eq. (26)) [9, 10].

$$Ma_L = \frac{d\sigma_L}{dx} \frac{\Delta x}{D_L \, \eta_L \, a} = \frac{d\sigma_L}{dx} \frac{x - x^*}{D_L \, \eta_L \, a} \frac{HTU_L}{HTU_{OL}} \tag{23}$$

$$\frac{HTU_L}{HTU_{OL}} = 1 - \frac{HTU_V}{HTU_{OV}} = \frac{X}{1 + X} \tag{24}$$

$$X = \frac{C_V}{C_L} m_{yx} \frac{M_L}{M_V} \frac{\varrho_V}{\varrho_L} \frac{\nu_L^{1/6}}{\nu_V^{5/12}} \frac{D_V^{2/3}}{D_L^{1/2}} \frac{a^{1/12}}{g^{1/6}} \frac{1}{(\varepsilon - h_L)^{1/2}} \frac{u_V^{3/4}}{u_L^{1/3}} \tag{25}$$

Table 2. *Capacity range and test facilities.*

		Loading-/flood point	Mass transfer
Gas capacity factor	F_V [$m^{-1/2} kg^{1/2} s^{-1}$]	0.47 ÷ 4.59	0.003 ÷ 2.77
Liquid load	u_L [$m^3/m^2 h$]	4.88 ÷ 144	0.256 ÷ 118
Liquid density	ϱ_L [kg/m^3]	750 ÷ 1026	758 ÷ 1237
Kinematic viscosity of liquid	ν_L [m^2/s] × 10^6	0.40 ÷ 104	0.30 ÷ 1.66
Surface tension of liquid	σ_L [kg/s^2] × 10^3	–	17.2 ÷ 74.0
Diffusion coefficient in liquid	D_L [m^2/s] × 10^9	–	1.04 ÷ 6.50
Gas density	ϱ_V [kg/m^3]	0.30 ÷ 1.37	0.07 ÷ 4.93
Kinematic viscosity of gas	ν_V [m^2/s] × 10^6	8.15 ÷ 41.5	2.20 ÷ 126
Diffusion coefficient in gas	D_V [m^2/s] × 10^6	–	3.70 ÷ 87.4
Investigated systems		13	45

$$\left(\frac{a_{Ph}}{a}\right)_{neg.sys.} = \left(\frac{a_{Ph}}{a}\right)_{Eq.(20)} (1 - 2.4 \times 10^{-4} |Ma_L|^{0.5}) \quad (26)$$

The term $d\sigma_L/dx$ in Eq. (23) describes the differential change in surface tension with the liquid concentration x; and the term Δx, the driving concentration difference from the liquid bulk to the phase boundary. The difference Δx is generally unknown; but, if the operating characteristic and equilibrium curve are known, it can be obtained from the overall difference $(x - x^*)$ and the distribution of the resistance to mass transfer HTU_L/HTU_{OL} (Eqs (24) and (25)). This is illustrated in Fig. 4, which shows an x-y diagram for the separation of a mixture by rectification. A detailed example is given in Refs [7, 9].

The gas stream exerts a strong effect on the liquid holdup above the loading point. Previous evaluations have revealed that the increase in h_L with the gas load, as represented in Fig. 1, can be expressed by Eq. (27) [8, 11]. The liquid holdup $h_{L,S}$ up to the loading point can be calculated from Eq. (18); and that at the flood point $h_{L,Fl}$ from Eq. (12).

$$h_L = h_{L,S} + (h_{L,Fl} - h_{L,S}) \left(\frac{u_V}{u_{V,Fl}}\right)^{1/3} \quad (27)$$

A change in film flow within the range above the loading point leads not only to an increase in the liquid holdup but also to an enlargement of the phase boundary. It is evident from observations at high gas loads in packed columns that, as the gas velocity increases, the film undulates or individual droplets are detached from it in the one layer of packing and regained by it in the overlying layer. Since no results of phase boundary measurements in this loading range have yet been published, it is assumed that, in analogy to Eq. (27), the area of the phase boundary, as defined by Eq. (28), tends towards a maximum at the flood point.

$$\frac{a_{Ph}}{a} = \frac{a_{Ph,S}}{a} + \left(\frac{a_{Ph,Fl}}{a} - \frac{a_{Ph,S}}{a}\right) \left(\frac{u_V}{u_{V,Fl}}\right)^{1/3} \quad (28)$$

The area of the phase boundary up to the loading point, expressed in terms of the area of the packing a, is independent of the gas velocity, i.e. $a_{Ph} = a_{Ph,S}$ and can be calculated from Eq. (20) or, if the system is negative, from Eq. (26).

The enlargement of the phase boundary and the increase in liquid holdup above the loading point are accompanied by back-mixing of the liquid caused by entrainment of liquid droplets in the gas stream. The shear stress in the countercurrent gas stream thus reduces the average effective velocity of the liquid film.

Eq. (4) describes the reduction of the average effective liquid velocity $\bar{u}_L$ with increase in gas load in the range between the loading and flood points in two-phase countercurrent flow. If the liquid holdup is introduced into this equation, Eq. (29) will be obtained.

$$\bar{u}_L = \frac{1}{3} g \varrho_L \frac{h_L^2}{a^2 \eta_L} - \frac{1}{4} \psi_L \frac{h_L}{(\varepsilon - h_L)^2} \frac{\varrho_V}{a \eta_L} u_V^2 \quad (29)$$

It can be seen that allowance must be made for the change in liquid holdup and in the resistance factor in calculating the average liquid velocity $\bar{u}_L$ above the loading point. Eq. (29) also indicates that the gas velocity $\bar{u}_V$ reduces the effective liquid velocity. For the determination of u_L above the loading point, an empirical equation (Eq. (30)) can be taken that describes in general the decrease in $\bar{u}_L$ in the $u_V \geq u_{V,S}$ range and contains the load-dependent quantities A and B.

$$\bar{u}_L = A - B (u_V - u_{V,S})^n \quad \text{if} \quad u_{V,S} \leq u_V \leq u_{V,Fl} \quad (30)$$

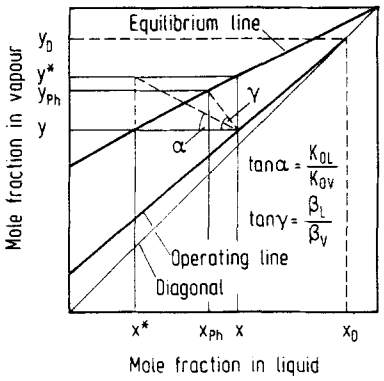

Fig. 4. *y-x*-concentration diagram to describe the overall concentration difference $(x - x^*)$ from equilibrium – and operating lines for determination of the Marangoni number, cf. Eq. (23).

The average effective liquid velocity up to the loading point is given by $\bar{u}_L = u_L/h_L$. Afterwards, it progressively decreases with an increase in the gas load until the flood point is reached, when it attains a value of zero as a result of strong back-mixing. Eq. (31) follows from these boundary conditions. (The exponent n is obtained from mass transfer experiments.)

$$\bar{u}_L = \frac{u_L}{h_L}\left\{1-\left(\frac{u_V-u_{V,S}}{u_{V,Fl}-u_{V,S}}\right)^2\right\} \quad \text{if} \quad u_{V,S} \le u_V \le u_{V,Fl} =$$

$$= \left(\frac{g\,\varrho_V^2\,u_V^2}{12\,\eta_L\,a^2\,\varrho_L}\right)^{1/3}\left(\frac{L}{V}\right)^{2/3}\left\{1-\left(\frac{u_V-u_{V,S}}{u_{V,Fl}-u_{V,S}}\right)^2\right\} \quad (31)$$

In the determination of the volumetric mass transfer coefficient on the liquid side, allowance must be made in accordance with Eq. (32) for the change in the average effective liquid load. The volumetric mass transfer coefficient on the gas side can be calculated by Eq. (33) with the liquid holdup determined from Eq. (27).

$$\beta_L\,a_{Ph} = C_L\,12^{1/6}\,\bar{u}_L^{1/2}\left(\frac{D_L}{d_h}\right)^{1/2} a\left(\frac{a_{Ph}}{a}\right) \quad (32)$$

$$\beta_V\,a_{Ph} = C_V\frac{1}{(\varepsilon - h_{L,\text{Eq. (27)}})^{1/2}}\frac{a^{3/2}}{d_h^{1/2}}D_V\left(\frac{u_V}{a\,\nu_V}\right)^{3/4}\times$$

$$\times\left(\frac{\nu_V}{D_V}\right)^{1/3}\left(\frac{a_{Ph}}{a}\right) \quad (33)$$

Typical results of mass transfer measurements including those performed at high column loads are shown in Fig. 5 for the vacuum rectification of a chlorobenzene/ethylbenzene mixture; in Fig. 6, for the absorption of ammonia from air in water; and in Fig. 7, for the desorption of carbon dioxide from water in air. Fig. 5 is characteristic for rectification: above the loading point, the specific efficiency NTU_{OV}/H initially increases until a maximum is attained and then decreases rapidly. In the absorption studies illustrated in Fig. 6, the specific number of transfer units decreases with the gas load and also passes through a minimum, after which it increases. In the desorption of carbon dioxide (Fig. 7), the gas load does not exert any effect at first on the specific efficiency NTU_L/H, because the resistance to mass transfer is entirely on the liquid side. It is only above the loading point that NTU_L/H increases.

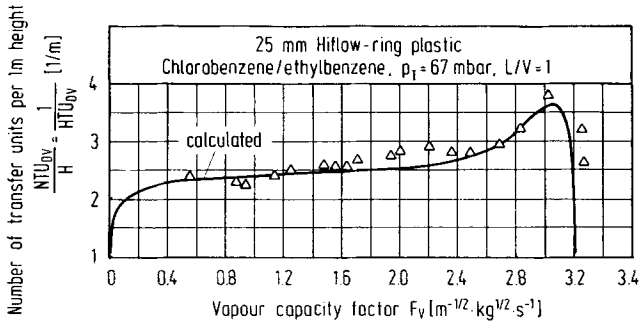

Fig. 5. Experimental and calculated specific efficiency NTU_{OV}/H for rectification under total reflux.

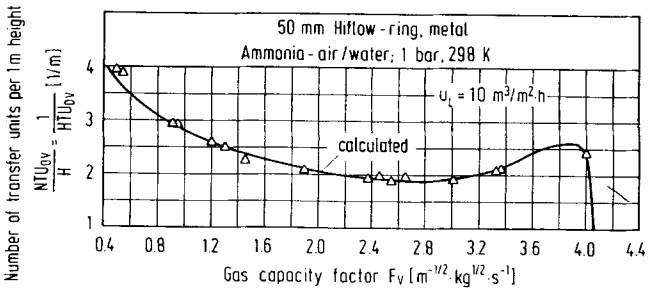

Fig. 6. Experimental and calculated specific efficiency NTU_{OV}/H for absorption as a function of gas capacity factor.

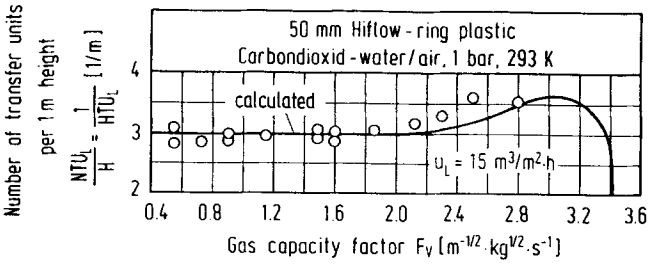

Fig. 7. Experimental and calculated specific efficiency NTU_L/H for desorption as a function of gas capacity factor.

Curves calculated from the above equations have been included in Figs 5 – 7. A balance that was made to minimize the difference between the experimental and calculated results yielded a value of $n = 2$ for the exponent n in Eq. (31) and demonstrated that the area of the phase boundary at the flood point could be described by Eq. (34),

$$\frac{a_{Ph,Fl}}{a} = 7\left(\frac{\sigma_L}{\sigma_W}\right)^{0.56}\frac{a_{Ph,S}}{a} =$$

$$= 10.5\left(\frac{\sigma_L}{\sigma_W}\right)^{0.56}(a\,d_h)^{-0.5}\,Re_{L,S}^{-0.2}\,We_{L,S}^{0.75}\,Fr_{L,S}^{-0.45} \quad (34)$$

where σ_L is the surface tension of the system and σ_W is the reference value of surface tension for water at 20 °C.

As can be seen from Figs 5 – 7, the values calculated from this function agree well with the experimental results. It is also evident that rectification represented the only case in which the flood point load was attained experimentally. As a consequence of pronounced back-mixing, the average effective liquid velocity $\bar{u}_L$ becomes zero at the flood point. The significance of this for mass transfer at the flood point is that the volumetric mass transfer coefficient on the liquid side also tends to zero and that the height of a transfer unit on the gas side, as defined by Eq. (22), becomes infinitely large or NTU_{OV}/H becomes infinitely small.

The absorption and desorption calculations reveal that a limit is imposed on the increase in NTU_{OV}/H or NTU_L/H

in the upper loading range and that, here too, the separation efficiency decreases considerably at the flood point. It can be derived from Figs 6 and 7 that the flood point was not reached in the absorption and desorption experiments.

It is evident that many factors affect mass transfer between the phase above the loading point. The greatly enlarged phase boundary in the upper loading range favours mass transfer on both the liquid and gas sides. Likewise, the increase in the liquid holdup leads to higher effective gas velocities, with the result that the volumetric mass transfer coefficient on the gas side becomes greater. Both these factors initially give rise to an increase in the separation efficiency of the equipment. It is only when the loads are close to the flood point that the liquid back-mixing brought about by entrained droplets events an influence on mass transfer that is sufficiently strong to overcompensate the effects mentioned and to cause a rapid decrease in separation efficiency after the maximum has been passed [11].

3 Conclusions

Equations for the determination of the loading and flood points were derived from a fluid dynamics model that describes two-phase countercurrent flow in packed columns in the loading range up to the flood point. It was demonstrated that mass transfer calculations must allow for the continuous decrease in the average effective liquid load at gas velocities above the loading point. In the upper loading range, both the liquid holdup and the area of the phase boundary increase and attain a maximum at the flood point.

It has been demonstrated that the values calculated from these equations closely agree with the results of rectification, absorption and desorption experiments performed in the total capacity range. All that is required for predicting performance are the properties of the phases, the loading parameters, and the data presented in Table 1 on specific types of packing.

Received: December 5, 1994 [CET 718]

Symbols used

a	[m^2/m^3]	surface area per unit packed volume
a_{Ph}	[m^2/m^3]	interfacial area per unit packed volume
C		constant
d_h	[m]	hydraulic diameter
d_S	[m]	column diameter
D	[m^2/s]	diffusion coefficient
F_V	[$m^{-1/2} kg^{1/2} s^{-1}$]	vapour or gas capacity factor
g	[m/s^2]	gravitational constant
H	[m]	height
h_L	[m^3/m^3]	liquid holdup
HTU	[m]	height of a mass transfer unit
HTU_O	[m]	overall height of a mass transfer unit
k_O	[m/s]	overall mass transfer coefficient
$\dot{L}$	[kmol/h]	molar flow of liquid
L	[kg/h]	mass flow of liquid
M	[kg/kmol]	molecular weight
m_{xy}	[kmol/kmol]	slope of the equilibrium line
n		exponent
N	[$1/m^3$]	packing density
NTU_O		overall number of transfer units
s	[m]	film thickness
u_L	[m^3/m^2 s]	superficial liquid load
$\bar{u}_L$	[m/s]	average effective liquid velocity
$\tilde{u}_{L,S}$	[m/s]	local liquid velocity
u_V	[m/s]	superficial gas or vapour velocity
$\bar{u}_V$	[m/s]	average effective gas or vapour velocity
$\dot{V}$	[kmol/h]	molar flow of gas or vapour
V	[kg/h]	mass flow of gas or vapour
x	[kmol/kmol]	mole fraction in liquid phase
y	[kmol/kmol]	mole fraction in gas or vapour phase

Greek symbols

β	[m/s]	mass transfer coefficient
ε	[m^3/m^3]	void fraction
η	[kg/m s]	dynamic viscosity
λ		stripping factor
ν	[m^2/s]	kinematic viscosity
ϱ	[kg/m^3]	density
σ	[kg/s^2]	surface tension
τ	[$kg/m\ s^2$]	shear stress
ψ		resistance coefficient

Subscripts

Fl	flood point
L	liquid
o	surface
Ph	interfacial
S	loading point
s	film thickness
V	vapour
W	water

Dimensionless numbers

Fr_L	Froude number of liquid
Ma_L	Marangoni number
Re_L	Reynolds number of liquid
We_L	Weber number of liquid

References

[1] Billet, R., *Industrielle Destillation*, Verlag Chemie, Weinheim 1973.

[2] Billet, R., *Festschrift der Fakultät für Maschinenbau*, Ruhr-Universität Bochum 1983, pp. 24 – 31.

[3] Billet, R., *I. Chem. E. Symp. Ser. No. 104* (1987) pp. A171 – A182.

[4] Billet, R., Schultes, M., *I. Chem. E. Symp. Ser. No. 104* (1987) pp. B255 – B266.

[5] Billet, R., *Chem. Eng. Technol. 11* (1988) pp. 139 – 148.

[6] Billet, R., *Fat. Sci. Technol. 92* (1990) pp. 361 – 370.

[7] Billet, R., Schultes M., *Beiträge zur Verfahrens- und Umwelttechnik*, Ruhr-Universität Bochum 1991, pp. 89 – 95.

[8] Billet, R., Schultes, M., *Chem. Eng. Technol. 14* (1991) pp. 89 – 95.

[9] Billet, R., Schultes, M., *Chem. Eng. Technol. 16* (1993) pp. 1 – 9.

[10] Schultes, M., *Ph. D. Thesis*, Ruhr-Universität Bochum 1990.

[11] Billet, R., *Packed Towers*, VCH Verlagsgesellschaft, Weinheim 1995.

Appendix

Numerical Example

Absorption of ammonia from 1500 m^3/h air with water at temperature of 25 °C under normal pressure in a packed column filled with 50 mm plastic Hiflow rings. The molar flow ratio of liquid/gas is 1.2 and the absorption column should operate at 80% of the capacity at the flood point.

The physical properties of gas/liquid-system

Molecular weight of gas	$M_V = 28.42$ kg/kmol
Molecular weight of liquid	$M_L = 18$ kg/kmol
Density of gas	$\varrho_V = 1.187$ kg/m^3
Density of liquid	$\varrho_L = 998$ kg/m^3
Viscosity of gas	$\eta_V = 18.75 \times 10^{-6}$ kg/ms
Viscosity of liquid	$\eta_L = 0.998 \times 10^{-3}$ kg/ms
Diffusion coefficient in gas	$D_V = 24.9 \times 10^{-6}$ m^2/s
Diffusion coefficient in liquid	$D_L = 2.01 \times 10^{-9}$ m^2/s
Surface tension of liquids	$\sigma_L = 72.14 \times 10^{-3}$ kg/s^2
Phase equilibrium of gas-liquid system	$m_{yx} = 0.95$

The characteristic packing data and constants:

Total surface area per unit volume	$a = 117.1$ m^2/m^3
Relative void fraction	$\varepsilon = 0.925$ m^3/m^3
Constants	$C_S = 2.894$
	$C_{Fl} = 1.871$
	$C_L = 1.487$
	$C_V = 0.345$

Operation data:

Volume stream of gas	$\dot{V} = 1500$ m^3/h
Molar flow ratio	$\dot{L}/\dot{V} = 1.2$
Specific gas velocity	$u_V = 0.8\, u_{V,Fl}$

The molar and mass flow of air and water is calculated by:

$$V = 1500 \frac{\text{m}^3}{\text{h}} 1.187 \frac{\text{kg}}{\text{m}^3} = 1780.5 \text{ kg/h}$$

$$\dot{V} = 1500 \frac{\text{m}^3}{\text{h}} \frac{1.187 \text{ kg/m}^3}{28.42 \text{ kg/kmol}} = 62.65 \text{ kmol/h}$$

$$\dot{L} = 1.2\, \dot{V} = 1.2\, 62.65 \frac{\text{kmol}}{\text{h}} = 75.18 \text{ kmol/h}$$

$$L = 75.18 \frac{\text{kmol}}{\text{h}} 18 \frac{\text{kg}}{\text{kmol}} = 1353.23 \text{ kg/h}$$

The column capacity at the loading point $u_{V,S}$ follows from Eqs (5) – (9) with the resistance factor ψ_S and the liquid holdup $h_{L,S}$.

For a flow parameter

$$\frac{L}{V}\sqrt{\frac{\varrho_V}{\varrho_L}} = \frac{1353.23}{1780.5}\left(\frac{1.187}{998}\right)^{1/2} = 0.026$$

less than 0.4 the exponent n_s is given by -0.326.

$$\xi_S = \frac{9.806}{2.894^2\left[\frac{1353.23}{1780.5}\left(\frac{1.187}{998}\right)^{1/2}\left(\frac{0.998\times10^{-3}}{18.75\times10^{-6}}\right)^{0.4}\right]^{2(-0.326)}} =$$

$$= 0.307$$

$$h_{L,S} = \left[\frac{12\ 0.998\times10^{-3}\ 117.1^2}{9.806\ 998} u_{L,S}\right]^{1/3}$$

$$u_{V,S} = \left(\frac{9.806}{0.307}\right)^{1/2}\left(0.925 - \left[\frac{120.998\times10^{-3}117.1^2}{9.806998} u_{L,S}\right]^{1/3}\right)\times$$

$$\times\left[\frac{12\ 0.998\times10^{-3}}{9.806\ 998\ 117.1} u_{L,S}\right]^{1/6}\left(\frac{998}{1.187}\right)^{1/2}$$

The liquid load $u_{L,S}$ is a function of gas velocity $u_{V,S}$ for constant mass flow ratio L/V

$$u_{L,S} = \frac{1353.23}{1780.5}\frac{1.187}{998} u_{V,S}$$

By iteration $u_{V,S}$ is calculated:

$$u_{V,S} = 2.470 \text{ m/s}$$

The gas velocity at flood point $u_{V,Fl}$ follows from Eqs (10) – (15) with the resistance factor ψ_{Fl} and the liquid holdup $h_{L,Fl}$. For the above determined flow parameter of $0.026 < 0.4$ the exponent n_{Fl} is given by -0.194.

$$\xi_{Fl} = \frac{9.806}{1.871^2\left[\frac{1353.23}{1780.5}\left(\frac{1.187}{998}\right)^{1/2}\left(\frac{0.998\times10^{-3}}{18.75\times10^{-6}}\right)^{0.2}\right]^{2(-0.194)}} =$$

$$= 0.928$$

$$h_{L,Fl}^3 (3\, h_{L,Fl} - 0.925) = \frac{6}{9.806}\frac{0.998\times10^{-3}}{998} 0.925\ 117.1^2 \times$$

$$\times \frac{1353.23}{1780.5}\frac{1.187}{998} u_{V,Fl}$$

$$u_{V,Fl} = \left(\frac{2\ 9.806}{0.928}\right)^{1/2}\frac{(0.925 - h_{L,Fl})^{3/2}}{0.925^{1/2}}\left(\frac{h_{L,Fl}}{117.1}\right)^{1/2} \times$$

$$\times\left(\frac{998}{1.187}\right)^{1/2}$$

The liquid load $u_{L,Fl}$ is again a function of the gas velocity $u_{V,Fl}$ for the mass flow ratio L/V.

$$u_{L,Fl} = \frac{1353.23}{1780.5}\frac{1.187}{998} u_{V,Fl}$$

Iteration gives the velocites at the flood point:

$$u_{V,Fl} = 3.442 \text{ m/s}$$

$$u_{L,Fl} = 3.113 \times 10^{-3} \text{ m}^3/\text{m}^2\text{s}$$

The absorption column should operate at 80% of the capacity at the flood point

$$u_V = 0.8\, u_{V,Fl} = 0.8\ 3.442 \text{ m/s} = 2.754 \text{ m/s}$$

$$u_L = \frac{1353.23}{1780.5}\frac{1.187}{998} u_V = 2.49 \times 10^{-3} \text{ m}^3/\text{m}^2\text{s}$$

The column diameter is then obtained

$$d_S = \sqrt{\frac{4}{\pi}\frac{V}{\varrho_V u_V}} = \sqrt{\frac{4}{\pi}\frac{1780.5/3600}{1.187\ 2.754}} = 0.44 \text{ m}$$

The liquid holdup at the loading and flood point for operating conditions are

$$h_{L,S} = \left(12\frac{0.998 \times 10^{-3}\ 2.49 \times 10^{-3}\ 117.1^2}{9.806\ 998}\right)^{1/3} = 0.0347$$

$$h_{L,Fl}^3 (3\, h_{L,Fl} - 0.925) = \frac{6}{9.81} 1 \times 10^{-6} 0.925\ 117.1^2 \times \times \frac{1353.23}{1780.5}\frac{1.187}{998} 2.754$$

By iteration the liquid holdup at the flood point is calculated for the boundary condition: $\varepsilon/3 < h_{L,Fl} < \varepsilon$

$$h_{L,Fl} = 0.309$$

so that the liquid holdup h_L follows from Eq. (27).

$$h_L = 0.0347 + (0.309 - 0.0347)\left(\frac{2.754}{3.442}\right)^{13} = 0.0497$$

The specific interfacial area at the loading and flood point for operating conditions is calculated with the hydraulic diameter of the packing d_h

$$d_h = 4\frac{0.925}{117.1} = 0.0316 \text{ m}$$

$$\frac{a_{Ph,S}}{a} = 1.5\,(117.1\ 0.0316)^{-0.5}\left(\frac{2.49 \times 10^{-3}\ 0.0316}{0.998 \times 10^{-3}/998}\right)^{-0.2} \times \times \left(\frac{(2.49 \times 10^{-3})^2\ 998\ 0.0316}{0.07214}\right)^{0.75} \times \times \left(\frac{(2.49 \times 10^{-3})^2}{9.806\ 0.0316}\right)^{-0.45} = 0.504$$

$$\frac{a_{Ph,Fl}}{a} = 7\left(\frac{0.07214}{0.0727}\right)^{0.56} 0.481 = 3.509$$

The specific interfacial area a_{Ph}/a follows then from Eq. (28).

$$\frac{a_{Ph}}{a} = 0.504 + (3.509 - 0.504)\left(\frac{2.754}{3.442}\right)^{13} = 0.668$$

Above the loading point, the effective liquid velocity $\bar{u}_L$ is reduced in form of Eq. (31)

$$\bar{u}_L = \frac{2.49 \times 10^{-3}}{0.0497}\left\{1 - \left(\frac{2.754 - 2.470}{3.442 - 2.470}\right)^2\right\} = 0.0458 \text{ m/s}$$

which effects the liquid side volumetric mass transfer coefficient in form of Eq. (32).

$$\beta_L a_{Ph} = 1.487\ 12^{1/6} 0.0458^{1/2}\left(\frac{2.01 \times 10^{-9}}{0.0316}\right)^{1/2} \times \times 117.1\ 0.668 = 9.51 \times 10^{-3} \text{ 1/s}$$

The gas side volumetric mass transfer coefficient is calculated from Eq. (33).

$$\beta_V a_{Ph} = 0.345\frac{1}{(0.925 - 0.0497)^{1/2}}\frac{117.1^{3/2}}{0.0316^{1/2}} 24.9 \times 10^{-6} \times \times \left(\frac{2.754\ 1.187}{117.1\ 18.75 \times 10^{-6}}\right)^{3/4} \times \times \left(\frac{18.75 \times 10^{-6}/1.187}{24.9 \times 10^{-6}}\right)^{1/3} 0.668 = 9.01 \text{ 1/s}$$

The heights of liquid and gas side mass transfer units are then

$$\text{HTU}_L = \frac{u_L}{\beta_L a_{Ph}} = \frac{2.49 \times 10^{-3}}{9.51 \times 10^{-3}} = 0.262 \text{ m}$$

$$\text{HTU}_V = \frac{u_V}{\beta_V a_{Ph}} = \frac{2.754}{9.01} = 0.306 \text{ m}$$

which give the following height of an overall gas side mass transfer unit with the stripping factor λ

$$\lambda = \frac{m_{yx}}{L/V} = \frac{0.95}{75.18/62.65} = 0.791$$

$$\text{HTU}_{OV} = \text{HTU}_V + \lambda\, \text{HTU}_L = 0.306 + 0.791\ 0.262 = = 0.512 \text{ m} .$$